Advection and dispersion of bedload tracers

E. Lajeunesse[1], O. Devauchelle[1], and F. James[2]

[1]Institut de Physique du Globe de Paris – Sorbonne Paris Cité, Équipe de Dynamique des Fuides Géologiques,
1 rue Jussieu, 75238 Paris cedex 05, France
[2]MAPMO UMR 7349 CNRS & Université d'Orléans, Fédération Denis Poisson FR CNRS 2964, Université d'Orléans, BP 6759, 45067 Orléans cedex 2, France

Correspondence to: E. Lajeunesse (lajeunes@ipgp.fr)

Abstract

We use the erosion-deposition model introduced by Charru et al. (2004) to simulate numerically the evolution of a plume of bedload tracers entrained by a steady flow. In this model, the propagation of the plume results from the stochastic exchange of particles between the bed and the bedload layer. We find a transition between two asymptotic regimes. At early time, the tracers, initially at rest, are gradually set into motion by the flow. During this entrainment regime, the plume, strongly skewed in the direction of propagation, continuously accelerates while spreading non-linearly. With time, the skewness of the plume eventually reaches a maximum value before decreasing. This marks the transition to an advection-diffusion regime in which the plume becomes increasingly symmetrical, spreads linearly, and advances at constant velocity. We derive analytically the expressions of the position, the variance and the skewness of the plume, and investigate their asymptotic regimes. Our model assumes steady state. In the field, however, bedload transport is intermittent. We show that the asymptotic regimes become insensitive to this intermittency when expressed in terms of the distance traveled by the plume. If this finding applies to the field, it might provide an estimate for the average bedload transport rate.

1 Introduction

Alluvial rivers transport the sediment that makes up their bed. From a mechanical standpoint, the flow of water applies a shear stress on the sediment particles, and entrains some of them downstream. When the shear stress is weak, the particles remain close to the bed surface as they travel (Shields, 1936). They roll, slide and bounce over the rough bed, until they settle down (Fernandez-Luque and Van Beek, 1976; Van Rijn, 1984; Nino and Garcia, 1994). This process is called bedload transport.

Bedload transport is inherently random (Einstein, 1937). A turbulent burst, or a collision with an entrained grain sometime dislodges a resting particle. The likeliness of this event depends on the specific arrangement of the surrounding particles. On average, however, the probability of entrainment is a function of macroscopic quantities such as shear stress and grain size (Ancey et al., 2008). Once dislodged, the velocity of a particle fluctuates significantly around its average (Lajeunesse et al.,

2010a; Furbish et al., 2012b, c, a; Roseberry et al., 2012). Finally, the particle's return to rest is yet another random event. Overall, a bedload particle spends only a small fraction of its time in motion.

Altogether, the combination of these stochastic processes results in a downstream flux of particles. Fluvial geomorphologists measure this flux by collecting moving particles in traps or Helley-Smith samplers (Leopold and Emmett, 1976; Helley and Smith, 1971). The instantaneous sediment discharge fluctuates due to the inherent randomness of bedload transport. However, averaging measurements over time yields a consistent sediment flux (Liu et al., 2008).

An alternative approach to sediment-flux measurements is to follow the fate of tracer particles. In November 1960, Sayre and Hubbell (1965) deposited 18 kg of radioactive sand in the North-Loup river, a sand-bed stream located in Nebraska (USA). Using a scintillator detector, they observed that the plume of radioactive sand gradually spread as it was entrained downstream. Tracking cobbles in gravel-bed rivers reveals a similar behavior: tracers disperse as they travel downstream (Bradley et al., 2010; Bradley and Tucker, 2012; Hassan et al., 2013; Phillips et al., 2013).

The dispersion of the tracers, expressed as the variance of their location, results from the randomness of bedload transport. Nikora et al. (2002) identify three regimes with distinct time scales. A particle entrained by the flow repeatedly collides with the bed (Lajeunesse et al., 2017). At short time, between two collisions, particles move with the flow, and the variance increases as the square of time (Martin et al., 2012; Fathel et al., 2016). This regime is analogous to the ballistic regime of Brownian motion (Zhang et al., 2012; Fathel et al., 2016).

As the particle continues its course, collisions deviate its trajectory. In this intermediate regime, the variance increases non-linearly with time (Martin et al., 2012). Nikora et al. (2002) attribute this behavior to anomalous super-diffusion; but Fathel et al. (2016) contest their interpretation.

With time, tracers settle back on the bed, where they can remain trapped for a long time. How the distribution of resting times influences the long-term dispersion of tracers remains unknown. The data collected by Sayre and Hubbell (1965) are consistent with the existence of a diffusive regime, in which the variance increases linearly (Zhang et al., 2012). Other investigators, however, report either subdiffusion or super-diffusion (Nikora et al., 2002; Bradley, 2017). These anomalous diffusion regimes are sometimes modeled with fractional advection-dispersion equations (Schumer et al., 2009; Ganti et al., 2010; Bradley et al., 2010).

The variability of the stream discharge further complicates the interpretation of field data. Bedload transport occurs when the shear stress exceeds a threshold set by the grain size. Most rivers fulfill this condition only a small fraction of the time, making sediment transport highly intermittent (Phillips et al., 2013; Phillips and Jerolmack, 2014). The rate at which tracers spread thus depends not only on the inherent randomness of bedload transport, but also on the probability distribution of the river discharge (Ganti et al., 2010; Phillips et al., 2013; Bradley, 2017).

Laboratory experiments under well-controlled conditions isolate these two effects. For instance, Lajeunesse et al. (2017) tracked a plume of dyed particles in an experimental channel. Although the flow was constant in this experiment, the tracers still dispersed as they traveled downstream. In this case, dispersion resulted from the inherent randomness of bedload transport only. We can decompose this randomness into two components. First, the velocity fluctuations disperse the particles (Furbish et al., 2012a, c, 2016). Secondly, the random exchange of particles between the bedload layer, where particles travel, and the

sediment bed, where particles are at rest, further disperses the particles (Lajeunesse et al., 2013, 2017). This effective diffusion also occurs in chromatography experiments, where a bonded phase exchanges the analyte with the flow (Van Genuchten and Wierenga, 1976).

In a recent paper, Lajeunesse et al. (2013) used the erosion-deposition model introduced by Charru et al. (2004) to derive the equations governing the evolution of a plume of tracers. Neglecting velocity fluctuations, they found that the second dispersion process, namely the exchange of particles between the bedload layer and the sediment bed, efficiently disperses the tracers. They also observed the transition between an initial transient and classical advection-diffusion. In the present paper, we further this investigation. Our objective is to derive formally the contribution of the advection-exchange of particles to the dispersion of a plume of tracers. To do so, we briefly rederive the equations governing the evolution of a plume of tracers (Sect. 2). We simulate numerically the propagation of a plume of tracers and discuss the nature of the two asymptotic regimes evidenced in Lajeunesse et al. (2013) (Sect. 3). We analyse the long-time advection-diffusion behavior of the plume and provide an analytical expression for the diffusion coefficient and the plume velocity (Sect. 4). We derive analytically the mean, the variance and the skewness of the tracers distribution and describe their asymptotic behavior in each regime (Sect. 5). Finally, we discuss the applicability of these results to the field (Sect. 6).

2   Entrainment of tracers

In most rivers, sediment are broadly distributed in size. This likely influences the dispersion of bedload tracers (Martin et al., 2012; Houssais and Lajeunesse, 2012; Pelosi et al., 2014). For the sake of simplicity, however, we restrict our analysis to a bed of uniform particles of size d_s. The bed is sheared by a flow, which applies a shear stress strong enough to entrain some particles. The latter remain confined in a thin bedload layer.

For moderate values of the shear stress, the concentration of moving sediments is small, and we can neglect the interactions between particles. The erosion-deposition model introduced by Charru et al. (2004) provides an accurate description of this dilute regime, in which bedload transport is controlled by the exchange of particles between the sediment bed and the bedload layer. This exchange sets the surface concentration of moving particles, n_{m}, through mass balance:

$$\frac{\partial n_{\mathrm{m}}}{\partial t} + V \frac{\partial n_{\mathrm{m}}}{\partial x} = E - D, \tag{1}$$

where we introduce the average particle velocity V. E is the erosion rate, defined as the number of bed particles set in motion per unit of time and area. Similarly, the deposition rate D is defined as the number of bedload particles settling on the bed per unit of time and area (Charru et al., 2004; Charru, 2006; Lajeunesse et al., 2010b; Seizilles et al., 2014; Lajeunesse et al., 2017).

To investigate the dispersion of bedload particles, we consider that some of them are marked (Fig. 1). We refer to these marked particles as "tracers", and assume that their physical properties are the same as those of unmarked particles. With these assumptions, the mass balance for the tracers in the bedload layer reads

$$n_{\mathrm{m}} \frac{\partial \phi}{\partial t} + n_{\mathrm{m}} V \frac{\partial \phi}{\partial x} = E \psi - D \phi \,, \tag{2}$$
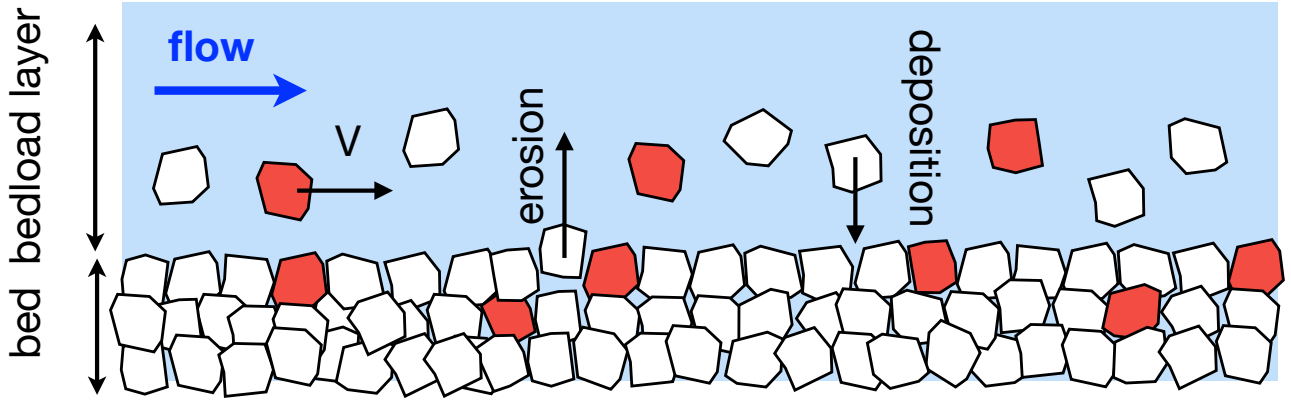
Figure 1. Granular bed sheared by a steady and uniform flow. The bed is a mixture of marked (red) and unmarked (white) grains.

where we introduce the proportion of tracers in the moving layer, ϕ. Similarly, ψ is the proportion of tracers on the bed surface.

When subjected to varying flow and sediment discharges, the bed of a stream accumulates or releases sediments (Gintz et al., 1996; Blom and Parker, 2004). Some particles may then be temporary buried within the bed, inducing streamwise dispersion (Crickmore and Lean, 1962; Pelosi et al., 2014). Here, we neglect this mechanism and restrict our analysis to steady 5 and uniform sediment transport. Accordingly, we assume that erosion and deposition affects the bed over a depth of about one grain diameter only. This hypothesis holds if the departure from the entrainment threshold is small enough. With these assumptions, the mass balance for the tracers on the bed surface reads

$$n_{\mathrm{s}}\frac{\partial \psi}{\partial t} = D\phi - E\psi \tag{3}$$

where n_s is the surface concentration of particles at rest on the bed surface. Each of them occupies an area of about d_s^2. The 10 surface concentration of particles at rest is therefore $n_s \sim 1/d_s^2$.

For steady and uniform transport, the surface concentration of moving particles, n, is constant. In addition, erosion and deposition balance each other:

$$E = D. \tag{4}$$

Laboratory experiments suggest that the deposition rate is proportional to the concentration of moving particles:

15 $$D = \frac{n_{\mathrm{m}}}{\tau_f} \tag{5}$$

where we introduce the average flight duration, $\tau_f = \ell_f/V$, and the average flight length, ℓ_f (Charru et al., 2004; Lajeunesse et al., 2010b). The flight length is the distance traveled by a mobile particle between its erosion and eventual deposition.

Similarly, the flight duration is the time a particle spends in the bedload layer. In practice, measuring these quantities often proves difficult, since they depend on how one defines the mobile and the static layer (Lajeunesse et al., 2017).

Combining equations (2), (3), (4) and (5) provides the set of equations that describe the propagation of the plume:

$$\frac{\partial \phi}{\partial t} + V \frac{\partial \phi}{\partial x} = \frac{1}{\tau_f}(\psi - \phi). \tag{6}$$

$$\frac{\partial \psi}{\partial t} = -\frac{\alpha}{\tau_f}(\psi - \phi) \tag{7}$$

where we define $\alpha = n_{\mathrm{m}}/n_{\mathrm{s}} \sim n_{\mathrm{m}}d_s^2$, the ratio of the concentration of moving particles to the concentration of static particles. This ratio is smaller than one. It is proportional to the intensity q_s of bedload transport:

$$\alpha \sim \frac{d_s^2}{V} q_s. \tag{8}$$

Complemented with initial and boundary conditions, equations (6) and (7) describe the evolution of the plume. In dimensionless form, they read

$$\frac{\partial \phi}{\partial \hat{t}} + \frac{\partial \phi}{\partial \hat{x}} = \psi - \phi \tag{9}$$

$$\frac{\partial \psi}{\partial \hat{t}} = -\alpha(\psi - \phi). \tag{10}$$

where $\hat{t} = t/\tau_f$ and $\hat{x} = x/\ell_f$ are dimensionless variables. For ease of notation, we drop the hat symbol in what follows.

A single parameter controls equations (9) and (10): the ratio of surface densities α, which characterizes the average distance between grains in the bedload layer. Since the erosion-deposition model assumes independent particles, we can only expect it to be valid when moving particles are sufficiently far away from each other, that is when α is small or, equivalently, when the Shields parameter is near threshold.

In the next section, we solve numerically equations (9) and (10).

3   Propagation of a plume of tracers

Laboratory measurements of bedload often use top-view images (Martin et al., 2012; Lajeunesse et al., 2017). Unless individual particles can be tracked, the tracers at rest are usually indistinguishable from those entrained by the flow. Separating the proportion of tracers in the moving layer, ϕ, from that on the bed surface, ψ, is practically impossible. Instead, top-view pictures show the total concentration of tracers:

$$c = \frac{n_m \phi + n_s \psi}{n_m + n_s} = \frac{\alpha}{\alpha + 1}\phi + \frac{1}{\alpha + 1}\psi. \tag{11}$$

Tracking sediment in rivers poses a similar problem. In general, one records the position of the tracers when the river stage is below the threshold of grain entrainment (Phillips et al., 2013; Phillips and Jerolmack, 2014). At the time of measurement, all tracers are therefore at rest. As a result, the proportion of mobile tracers vanishes ($\phi = 0$), and the total concentration of tracers reads $c = \psi/(\alpha + 1)$.

In summary, the proportions of mobile and static tracers, ϕ and ψ, naturally derive from mass balance (2) and (3). However their measurement proves difficult during active transport. On the other hand, experimental and field investigations provide the total concentration of tracers, c (Sayre and Hubbell, 1965; Lajeunesse et al., 2017). This quantity is conservative, as the total amount of tracers, $M = \int c\,\mathrm{d}x$, is preserved. In the following, we therefore focus on the concentration of tracers, c.

To study the evolution of the tracer concentration, we solve equations (9) and (10) numerically, using a finite volume scheme. We then compute the tracer concentration using equation (11) (Fig. 2).

The early evolution of the plume depends on initial conditions. In most field experiments, tracers are deposited at the surface of the river bed when the flow stage is low and sediment are motionless (Phillips et al., 2013). During floods, the river discharge increases and the shear stress eventually exceeds the entrainment threshold, setting in motion some of the grains. The entrainment of particles strongly depends on the arrangement of the bed: grains highly exposed to the flow move first (Charru et al., 2004; Turowski et al., 2011; Agudo and Wierschem, 2012). Several authors find that the tracers they disposed on the bed are more mobile during the first flood than during later ones (Bradley and Tucker, 2012). During the later floods, tracers gradually get trapped in the bed, and their average mobility decreases. On the other hand, Phillips and Jerolmack (2014) find no special mobility during the first flood. In the absence of a clear scenario, we choose the simplest possible initial conditions: we assume that, initially, all tracers belong to the static layer: $\phi(x, t = 0) = 0$.

With these initial conditions, the evolution of the plume follows two distinct regimes. At early times, the flow gradually dislodges tracers from the bed and entrains them in the bedload layer. During this entrainment regime, only a small proportion of the tracers move. Consequently, the plume develops a thin tail in the downstream direction (Fig. 2a). The corresponding distribution of travel distances is strongly skewed towards the direction of propagation, a feature commonly observed in field experiments (Liébault et al., 2012; Phillips and Jerolmack, 2014).

With time, the plume moves downstream and spreads both upstream and downstream. As a result, the concentration rapidly decreases to small levels. The plume becomes gradually symmetrical and tends asymptotically towards a Gaussian distribution (Fig. 2b). This regime is reminiscent of classical diffusion.

To better illustrate this evolution, we introduce the mean position of the plume of tracers:

$$\langle x \rangle = \frac{1}{M} \int_{-\infty}^{\infty} c\,x\,\mathrm{d}x. \tag{12}$$

We also characterize its size with the variance:

$$\sigma^2 = \frac{1}{M} \int_{-\infty}^{\infty} c\,(x - \langle x \rangle)^2\,\mathrm{d}x \tag{13}$$

and its symmetry with the skewness:

$$\gamma = \frac{1}{M} \int_{-\infty}^{\infty} c\left(\frac{x - \langle x \rangle}{\sigma}\right)^3\,\mathrm{d}x. \tag{14}$$

The evolution of these three moments is consistent with the existence of two asymptotic regimes (Fig. 3). At short time, the plume grows a thin tail downstream. This deformation causes the plume's skewness to increase as t^4. During this regime, the
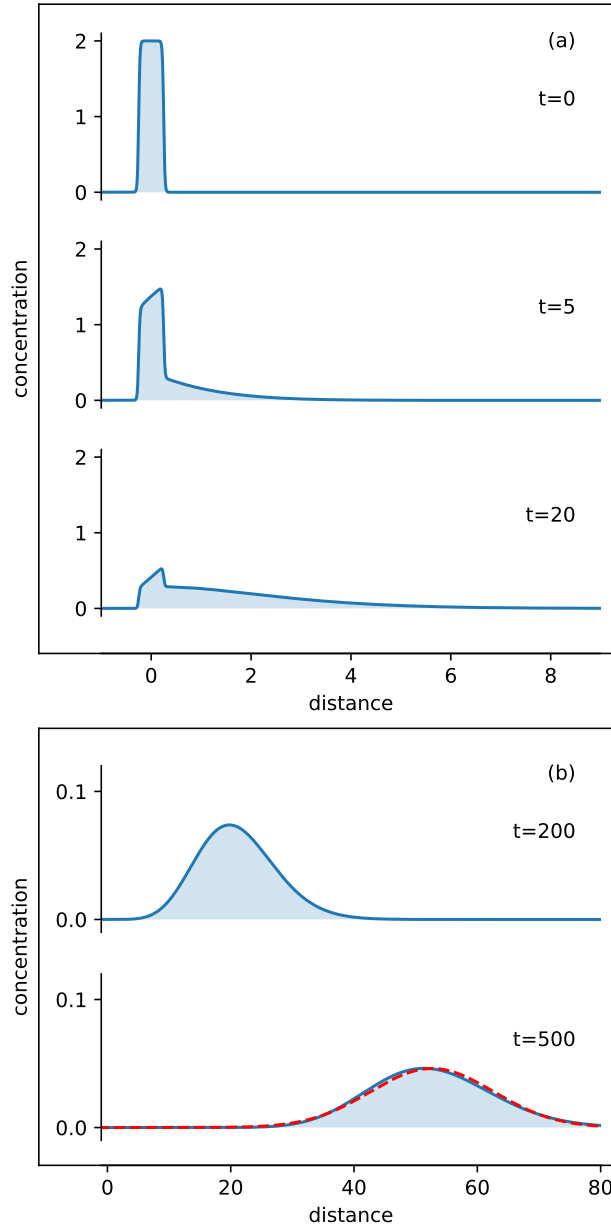
Figure 2. Evolution of the tracer concentration ($\alpha = 0.1$) obtained by solving numerically equations (9) and (10). (a) Early entrainment regime. (b) Relaxation towards the diffusive regime. Tracers are initially at rest, forming a symmetric plume of length $L = 0.5$ and mass $M = 1$. The concentration profile asymptotically tends towards a Gaussian distribution (dotted red line).

average location of the plume increases as t^2 and its variance grows as t^3. Although the variance increases non-linearly with time, the exponent, 3, is too large for super-diffusion (Weeks and Swinney, 1998).

After a characteristic time of the order of $\tau \approx \tau_f$, the skewness of the plume reaches a maximum (Fig. 3c). This corresponds to a drastic change of dynamics: the skewness starts decreasing as the plume becomes gradually more symmetrical. At long time, the plume of tracers advances at constant velocity and diffuses linearly with time (Fig. 3a and b). This regime, regardless of the value of α, corresponds to classical advection-diffusion.

5   Next, we establish the equivalence between diffusion and the long-time behavior of the tracers.

4   Advection-diffusion at long time

The diffusion at work in equations (9) and (10) results from the continuous exchange of particles between the bedload layer, where particles travel at the constant velocity V, and the sediment bed, where particles are at rest. The velocity difference between the two layers gradually smears out the plume and spreads it in the flow direction. This process occurs in a variety of physical systems in which layers moving at different velocities exchange a passive tracer. A typical example is Taylor dispersion, where a passive tracer diffuses across a Poiseuille flow in a circular pipe (Taylor, 1953). The combination of shear rate and transverse molecular diffusion generates an effective diffusion in the flow direction. Other exemples of effective diffusion include solute transport in porous media and chromatography (Van Genuchten and Wierenga, 1976).

To establish formally the equivalence between diffusion and the long-time behavior of the plume, we follow a reasoning similar to the one developed for chromatography (James et al., 2000). Equations (9) and (10) are equivalent to:

$$\frac{\partial c}{\partial t} + \frac{\alpha}{\alpha+1}\frac{\partial c}{\partial x} = \frac{\alpha}{(\alpha+1)^2}\frac{\partial \delta}{\partial x}, \tag{15}$$

$$\frac{\partial \delta}{\partial t} + \frac{1}{\alpha+1}\frac{\partial \delta}{\partial x} + (\alpha+1)\delta = \frac{\partial c}{\partial x}, \tag{16}$$

where we introduce $\delta = \psi - \phi$, the difference between the proportion of tracers on the sediment bed and that in the bedload layer. Eventually, these proportions equilibrate each other. At long time, we therefore expect the solution of equations (15) and (16) to relax towards steady state, for which δ is of order $\epsilon \ll 1$. Accordingly, we rewrite these two equations as

$$\frac{\partial c}{\partial t} + \frac{\alpha}{\alpha+1}\frac{\partial c}{\partial x} = \epsilon \frac{\alpha}{(\alpha+1)^2}\frac{\partial \delta}{\partial x}, \tag{17}$$

$$\frac{\partial \delta}{\partial t} + \frac{1}{\alpha+1}\frac{\partial \delta}{\partial x} + (\alpha+1)\,\delta = \frac{1}{\epsilon}\frac{\partial c}{\partial x}. \tag{18}$$

Introducing $T = \epsilon\, t$ and $X = \epsilon\, x$, and developing c and δ with respect to ϵ yields

$$\frac{\partial c_0}{\partial T} + \frac{\alpha}{\alpha+1}\frac{\partial c_0}{\partial X} = 0 \tag{19}$$

$$(\alpha+1)\,\delta_0 = \frac{\partial c_0}{\partial X} \tag{20}$$

at zeroth order, and

$$\frac{\partial c_1}{\partial T} + \frac{\alpha}{\alpha+1}\frac{\partial c_1}{\partial X} = \frac{\alpha}{(\alpha+1)^2}\frac{\partial \delta_0}{\partial X} \tag{21}$$

at first order.
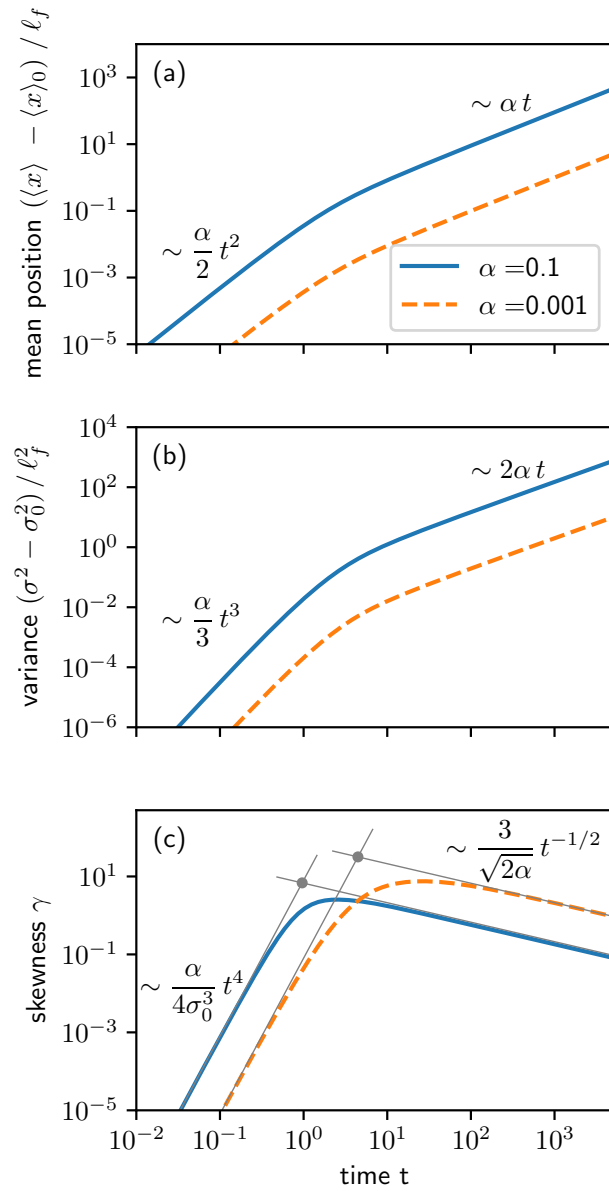
Figure 3. (a) Position, (b) variance and (c) skewness of a plume of tracers as a function of time for $\alpha = 0.1$ and $\alpha = 0.001$. We compute the evolution of these three quantities using equations (28), (33) and (38). The results agree exactly with numerical simulations. The asymptotic regimes of the skewness are represented with grey lines. Their intersection provides an estimate of the duration of the entrainment regime (see equation (45)).

Multiplying equation (21) by ϵ and summing the result with equation (19), we finally get

$$\frac{\partial c}{\partial t} + \frac{\alpha}{\alpha+1} \frac{\partial c}{\partial x} = \frac{\alpha}{(\alpha+1)^3} \frac{\partial^2 c}{\partial x^2}. \tag{22}$$

At long time, the transport of the tracers follows the advection-diffusion equation (22). We identify the advection velocity, U, which reads:

$$U = \frac{\alpha}{\alpha+1} \frac{\ell_f}{\tau_f} \sim \alpha \frac{\ell_f}{\tau_f}, \tag{23}$$

Likewise, the diffusion coefficient reads:

$$C_d = \frac{\alpha}{(\alpha+1)^3} \frac{\ell_f^2}{\tau_f} \sim \alpha \frac{\ell_f^2}{\tau_f}. \tag{24}$$

This asymptotic equivalence explains the advection-diffusion regime (Figures 2 and 3).

We interpret this formal derivation as follows. In the reference frame of the plume, a tracer at rest on the bed moves backward, while a tracer entrained in the bedload layer moves forward. At long time, the proportions of tracers in each layer equilibrate. Consequently, the probability that a tracer be entrained and move forward, equals that of deposition. In the reference frame of the plume, the exchange of particles between the bed and the bedload layer is thus a Brownian motion, hence the linear diffusion of the plume.

In the next section, we investigate the evolution of the location, the size and the symmetry of the plume as it propagates downstream.

5   Location, size and symmetry of the plume

Concentration, defined as the number of tracers per unit of area, depends on the area over which it is measured. Its value is meaningful when the measurement area is much larger than the distance between particles, and much smaller than the plume. During the entrainment regime, the plume develops a thin tail containing only a small proportion of tracers. Measuring the concentration profile during this regime is thus challenging. To our knowledge, only Sayre and Hubbell (1965) were able to measure consistent concentration profiles, using radioactive sand. In practice, most field campaigns involve a limited number of tracers (900 at most) (Liébault et al., 2012; Bradley and Tucker, 2012; Phillips and Jerolmack, 2014; Bradley, 2017). It is thus more practical to consider integral quantities, such as the mean position of the plume $\langle x \rangle$, its variance σ^2, and its skewness γ.

Multiplying equation (15) by x and integrating over space provides the evolution equation for the mean position:

$$\frac{\partial \langle x \rangle}{\partial t} = \frac{\alpha}{\alpha+1} - \frac{\alpha}{(\alpha+1)^2} \langle \delta \rangle \tag{25}$$

where

$$\langle \delta \rangle = \frac{1}{M} \int \delta \, dx \tag{26}$$

is the average difference between the proportion of tracers on the sediment bed and in the bedload layer. To solve equation (25), we need an equation for $\langle \delta \rangle$. The latter is obtained by integrating (16) over space:

$$\frac{\partial \langle \delta \rangle}{\partial t} = -(\alpha + 1) \langle \delta \rangle \tag{27}$$

Equations (25) and (27) describe the downstream motion $\langle x \rangle$ of the plume. To solve them, we need to specify initial conditions. As discussed in section 3, we consider that all tracers initially belong to the static layer i.e. $\phi(x, t = 0) = 0$. This condition and the conservation of mass, $\langle c \rangle = 1$, provide initial conditions for $\langle \delta \rangle$: $\langle \delta \rangle (t = 0) = \alpha + 1$. With this condition, equations (25) and (27) integrate into

$$\langle x \rangle - \langle x \rangle_0 = \frac{\alpha}{\alpha + 1} t + \frac{\alpha}{(\alpha + 1)^2} \left(e^{-(\alpha + 1)t} - 1 \right) \tag{28}$$

where $\langle x \rangle_0$ is the initial position of the plume.

We now focus on the variance of the plume. Multiplying (15) by x^2 and integrating over space yields the evolution equation for the second moment of the tracer distribution:

$$\frac{\partial \langle x^2 \rangle}{\partial t} = \frac{2\alpha}{(\alpha + 1)} \langle x \rangle - \frac{2\alpha}{(\alpha + 1)^2} \langle x\delta \rangle \tag{29}$$

where

$$\langle x\,\delta \rangle = \frac{1}{M} \int x\,\delta\,dx. \tag{30}$$

is the first moment of δ. To solve equation (29), we need an equation for this intermediate quantity. We obtain it by multiplying (16) by x and integrating over space:

$$\frac{\partial \langle x\delta \rangle}{\partial t} = -1 - (\alpha + 1)\langle x\delta \rangle + \frac{\langle \delta \rangle}{\alpha + 1} \tag{31}$$

At time $t = 0$, $\langle x\delta \rangle (t = 0) = (\alpha + 1)\langle x \rangle_0$. Equations (29) and (31) with this initial condition provide the expression of the second moment of the tracer distribution:

$$\langle x^2 \rangle = \langle x^2 \rangle_0 + \frac{2\,\alpha}{(\alpha + 1)^3} \left(t + \frac{2 - \alpha}{\alpha + 1} \right) e^{-(\alpha + 1)t} + \frac{\alpha^2}{(\alpha + 1)^2} t^2$$
$$+ \frac{2\alpha\,(1 - \alpha)}{(\alpha + 1)^3} t + \frac{2\alpha\,(\alpha - 2)}{(\alpha + 1)^4} \tag{32}$$

where $\langle x^2 \rangle_0$ is the initial value of the second moment of the tracer distribution. We then deduce the variance of the plume from:

$$\sigma^2 = \langle x^2 \rangle - \langle x \rangle^2. \tag{33}$$

We follow a similar procedure to derive the skewness of the plume. Multiplying (15) by x^3 and integrating over space yields the evolution equation for the third moment of the tracer distribution:

$$\frac{\partial \langle x^3 \rangle}{\partial t} = \frac{3\alpha}{(\alpha + 1)} \langle x^2 \rangle - \frac{3\alpha}{(\alpha + 1)^2} \langle x^2\delta \rangle \tag{34}$$

where

$$\langle x^2 \delta \rangle = \frac{1}{M} \int x^2 \delta \, dx. \tag{35}$$

is the second moment of δ. Multiplying (16) by x^2 and integrating over space provides the evolution equation for this intermediate quantity:

$$\frac{\partial \langle x^2 \delta \rangle}{\partial t} = -(\alpha+1)\langle x^2 \delta \rangle + \frac{2}{\alpha+1}\langle x \delta \rangle - 2\langle x \rangle \tag{36}$$

At time $t = 0$, $\langle x^2 \delta \rangle = (\alpha+1)\langle x^2 \rangle_0$ and $\langle x^3 \rangle = 0$. With these initial conditions, equations (34) and (36) provide the expression of $\langle x^3 \rangle$:

$$\langle x^3 \rangle = \frac{3\alpha}{\alpha+1} \left(\sigma_0^2 + \frac{2\alpha^2 - 8\alpha + 2}{(\alpha+1)^4} \right) t$$

$$+ \frac{3\alpha}{(\alpha+1)^2} \left(\sigma_0^2 + \frac{2\alpha^2 - 12\alpha + 6}{(\alpha+1)^4} \right) \left(e^{-(\alpha+1)t} - 1 \right)$$

$$+ \frac{3\alpha}{(\alpha+1)^4} \left(t - 4\frac{\alpha-1}{\alpha+1} \right) t \, e^{-(\alpha+1)t}$$

$$+ \frac{\alpha^3}{(\alpha+1)^3} \left(t - \frac{3(\alpha-2)}{\alpha(\alpha+1)} \right) t^2 \tag{37}$$

from which we deduce the skewness of the plume:

$$\gamma = \frac{\langle x^3 \rangle - 3 \langle x \rangle \, \sigma^2 - \langle x \rangle^3}{\sigma^3} \tag{38}$$

Equations (28), (32), (33), (37), and (38) represent the evolution of the mean, the variance and the skewness of the tracers distribution, that is, its migration, spreading and symmetry. They do not require any assumption, other than the ones of the model itself, and agree exactly with numerical simulations (Fig. 3).

As discussed in section 3, numerical simulations reveal a transient during which the tracers, initially at rest, are gradually set into motion by the flow (Fig. 3). During this entrainment regime, the plume continuously accelerates, spreads non-linearly and becomes increasingly asymmetrical. To characterize this regime, we expand equations (28), (32), (33), (37), and (38) to leading order in time:

$$\langle x \rangle - \langle x \rangle_0 \quad \sim \quad \frac{\alpha}{2} \, t^2 \tag{39}$$

$$\sigma^2 - \sigma_0^2 \quad \sim \quad \frac{\alpha}{3} \, t^3 \tag{40}$$

$$\gamma \quad \sim \quad \frac{\alpha}{4 \, \sigma_0^3} \, t^4. \tag{41}$$

These three equations are consistent with our numerical simulations (Fig. 3).

Anomalous diffusion arises from heavy-tailed distributions, of either the step length or the waiting time (Weeks and Swinney, 1998). The erosion-deposition model contains no such ingredient. Here the fast increase of the variance results from the exchange of particles between the sediment bed and the bedload layer, at the beginning of the experiment. Over a time shorter

than the flight duration τ_f, the tracers entrained by the flow do not settle back on the bed. They form a thin tail, which leaves the main body of the plume, and moves downstream at the average particle velocity V (Fig. 2a). The plume therefore consists of a main body of virtually constant concentration, followed by a thin tail of length $\propto Vt$. Accordingly, we can split the integral that defines its mean position, equation (12), into two terms. The first one, obtained by integrating cx over the main body of the plume, yields the initial position of the plume $\langle x \rangle_0$. The second one, obtained by integrating cx over a tail of length Vt, scales as t^2. Summing these contributions yields equation (39). Similar reasonings yield equations (40) and (41) for the variance and the skewness.

With time, the plume enters the diffusive regime. Its velocity and its spreading rate relax towards constants while its skewness decreases (Fig. 3). We derive the corresponding asymptotic behavior by expanding equations (28), (32), (33), (37), and (38) at long time:

$$\langle x \rangle - \langle x \rangle_0 \quad \sim \quad \frac{\alpha}{\alpha + 1}\, t \sim \alpha\, t \tag{42}$$

$$\sigma^2 - \sigma_0^2 \quad \sim \quad 2\frac{\alpha}{(\alpha + 1)^3}\, t \sim 2\,\alpha\, t \tag{43}$$

$$\gamma \quad \sim \frac{3}{\sqrt{2\,\alpha}}\, \frac{1}{\sqrt{t}} \tag{44}$$

The asymptotic regimes (42) and (43) are consistent with the expressions derived in section 4.

The transition between the entrainment and the diffusive regime occurs when the skewness reaches its maximum value. Equating the skewness estimated from (41) and (44) provides the approximate duration of the entrainment regime, τ. We find

$$\tau_e = (72)^{1/9} \left(\frac{\sigma_0^2}{\alpha} \right)^{1/3} \tau_f \tag{45}$$

which compares well with our numerical simulations (Fig. 3). The duration of the entrainment regime increases with the initial size of the plume and decreases with the intensity of sediment transport.

The asymptotic regimes (39), (40), (41), (42), (43) and (44) assume that sediment transport is in steady state. In the next section, we discuss the intermittency of bedload transport in natural streams.

6 Intermittency of bedload transport

Our description of the plume of tracers is based on the assumption that sediment transport is in steady state. This hypothesis is often satisfied in laboratory flumes (Lajeunesse et al., 2017). In a river, it may be met for up to a few days (Sayre and Hubbell, 1965). At longer time scales, however, most rivers alternate between low-flow stages during which sediment is immobile, and floods, during which bed particles are entrained downstream (Phillips and Jerolmack, 2016). Bedload transport is thus intermittent.

The intermittency of bedload transport influences the propagation of tracers in several ways. First of all, sediment transport during a flood modifies the structure of the bed (Lenzi et al., 2004; Turowski et al., 2009, 2011). As a result, the proportion of tracers in the bedload layer and in the bed, ϕ and ψ, likely change from one flood to the next. In a effort to address this
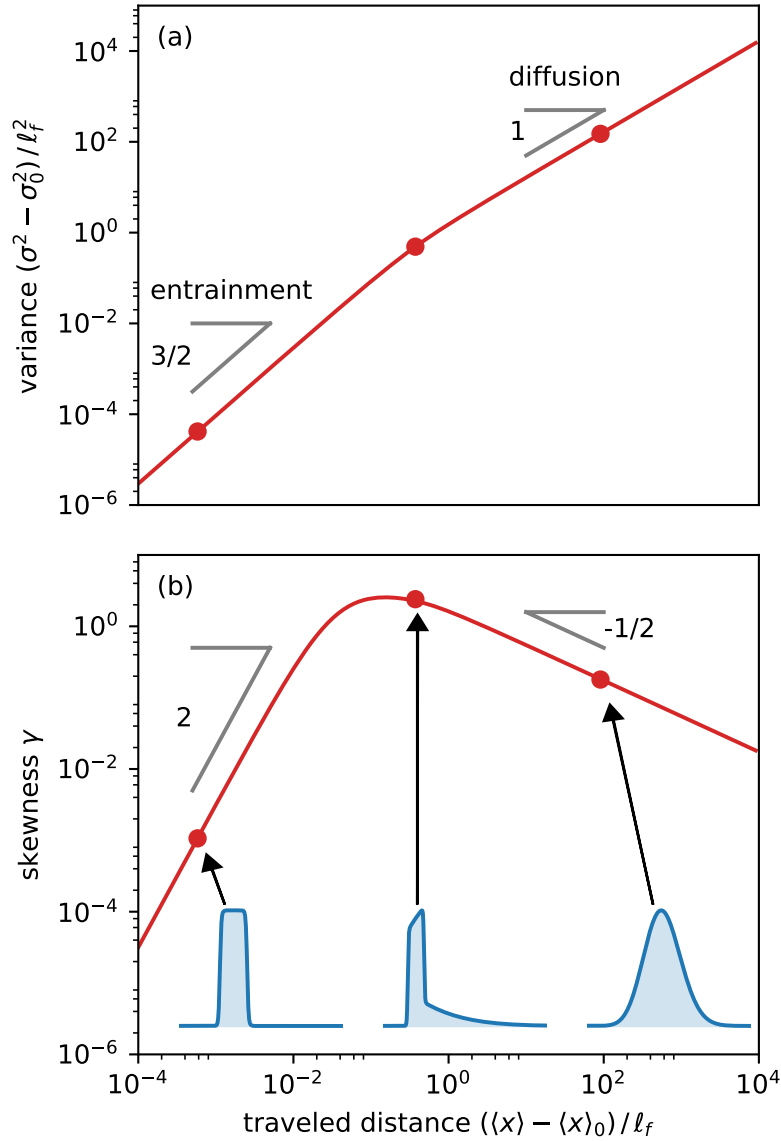
Figure 4. (a) Variance and (b) skewness of a plume of tracers as a function of traveled distance ($\alpha = 0.1$). These three quantities are calculated from equations (28), (33) and (38). Inset: concentration profiles (blue) illustrating the shape of the plume during the entrainment regime, at the transition between the entrainment and the diffusive regime and in the diffusive regime.

question, P. Allemand and collaborators recently implemented the survey of a river located in Basse-Terre Island (Guadeloupe

archipelago). Their preliminary observations reveal that the cobbles deposited at the end of a flood are the first entrained at the beginning of the next (P. Allemand, personal communication, June 30, 2017). Based on this observation, we speculate that a tracer belonging to the bedload layer at the end of a flood will still be part of the bedload layer at the beginning of the next one. Similarly, a tracer locked in the bed at the end of a flood will belong to the static layer at the beginning of the next one. In other words, we assume that tracers freeze between two floods.

If this assumption holds, the simplest way to account for bedload intermittency is to assume that the river alternates between two representative stages: 1) a low-flow stage during which tracers are immobile; 2) a flood stage, characterized by a representative sediment flux $q_s \sim \alpha V/d_s^2$, during which tracers propagate downstream (Paola et al., 1992; Phillips et al., 2013). Following this model, we may extrapolate our results to the field, provided we rescale time with respect to an intermittency factor $I = T_e/T$, where T is the total duration of elapsed time, while T_e is the time during which sediments are effectively in motion (Paola et al., 1992; Parker et al., 1998; Phillips et al., 2013).

In practice, evaluating the intermittency factor requires continuous monitoring of the river discharge, and a correct estimate of the entrainment threshold. Liébault et al. (2012), for instance, monitored the location of tracer cobbles deposited in the Bouinenc stream (France) during 2 years. Over this period, the motion of the tracers resulted from 55 floods, for a total duration of 42 days. Sediments were thus in motion less than $I = 12\%$ of the time.

Here, we suggest another way to circumvent the intermittency of sediment transport. Plotting the plume variance, $(\sigma^2 - \sigma_0^2)$, and its skewness, γ, as a function of traveled distance, $\langle x \rangle - \langle x \rangle_0$, eliminates time from the equations (Fig. 4). In this plot, the position of the plume acts as a proxy for the effective duration of sediment transport, T_e. The resulting curves are thus filtered from transport intermittency (Fig. 4).

The entrainment regime corresponds to small traveled distances. In this regime, both the size of the plume and its asymmetry increase with traveled distance (Fig. 4). Equations (39), (40) and (41) describe the early evolution of the plume. Eliminating time by combining them, we find the behavior of the plume for short traveled distances:

$$\sigma^2 - \sigma_0^2 = \sqrt{\frac{8\,\ell_f}{9\,\alpha}}\,\left(\langle x \rangle - \langle x \rangle_0\right)^{3/2}, \tag{46}$$

$$\gamma = \frac{\ell_f}{\alpha\,\sigma_0^3}\,\left(\langle x \rangle - \langle x \rangle_0\right)^2. \tag{47}$$

As discussed in section 5, these scalings result from the gradual entrainment of the tracers that are initially trapped in the bed.

After the plume has traveled over a distance roughly equal to the flight length, its skewness reaches a maximum value and starts decreasing. This change of dynamics indicates the transition towards the diffusive regime. Equations (42), (43) and (44) provide the long-term behavior of the plume :

$$\sigma^2 - \sigma_0^2 \sim 2\,\ell_f\,\left(\langle x \rangle - \langle x \rangle_0\right), \tag{48}$$

$$\gamma = \frac{3}{\sqrt{2}}\,\sqrt{\frac{\ell_f}{\langle x \rangle - \langle x \rangle_0}}. \tag{49}$$

The linear increase of the variance with the distance traveled by the plume is the signature of standard diffusion (see section 5).

Equating the skewness estimated from (47) and (49) provides the position $\langle x \rangle_{max}$ at which the skewness reaches its maximum:

$$5 \quad \langle x \rangle_{max} - \langle x \rangle_0 \sim \left(\frac{3\,\alpha}{\sqrt{2}} \right)^{2/5} \left(\frac{\sigma_0^6}{\ell_f} \right)^{1/5}. \tag{50}$$

The entrainment regime lasts until the plume has traveled over a distance comparable to its initial size, that is until $\langle x \rangle - \langle x \rangle_0 \sim \sigma_0$.

When expressed in terms of the distance traveled by the plume, the asymptotic regimes are insensitive to the intermittency of bedload transport. They are thus a robust test of our model, and can help us interpret field data. Let us assume that a dataset
10   records the evolution of a plume of tracers released in a river, over a distance long enough to explore both the entrainment and the diffusive regime. During the diffusive regime, the skewness decreases with the traveled distance. A fit of the data with equation (49) yields the flight length, ℓ_f. Knowing the latter, we could use equation (47) to estimate the intensity of sediment transport, α, from the evolution of the skewness during the entrainment regime.

According to section 5, the skewness reaches a maximum after a time τ_e (equation (45)). Taking into account the intermit-
15   tency of bedload transport in natural streams, we expect that this maximum is reached when

$$t = (72)^{1/9} \left(\frac{\sigma_0^2}{\alpha} \right)^{1/3} \frac{\tau_f}{I}, \tag{51}$$

where I is the intermittency factor. Identifying this maximum in a field experiment thus yields the ratio τ_f/I. Combining the latter with our estimates of the flight length, ℓ_f, and the intensity of sediment transport, α, should provide us with the average sediment transport rate in the river:

$$20 \quad \bar{q}_s = I\,\alpha\,d_s^2\,\frac{l_f}{\tau_f}. \tag{52}$$

7   Conclusion

We used the erosion-deposition model introduced by Charru et al. (2004) to describe the evolution of a plume of bedload tracers entrained by a steady flow. In this model, the propagation of the plume results from the stochastic exchange of particles between the bed and the bedload layer. This mechanism is reminiscent of the propagation of tracers in a porous medium (Berkowitz and
25   Scher, 1998). The evolution of the plume depends on two control parameters: its initial size, σ_0 , and the intensity of sediment transport, α.

Our model captures in a single theoretical framework the transition between two asymptotic regimes : 1) an early entrainment regime during which the plume spreads non-linearly, 2) a late-time relaxation towards classical advection-diffusion. The latter regime is consistent with previous observations (Nikora et al., 2002; Zhang et al., 2012).

When expressed in terms of the distance traveled by the plume, the asymptotic regimes are insensitive to the intermittency of bedload transport in natural streams. According to this model, it should be possible to estimate the particle flight length and the average bedload transport rate from the evolution of the variance and the skewness of a plume of tracers in a river.

Acknowledgements. It is our pleasure to thank P. Allemand, D. Furbish, C. Phillips, D. Jerolmack and F. Métivier for many helpfull and enjoyable discussions. This work was supported by the French national programme EC2CO-Biohefect/Ecodyn//Dril/MicrobiEn, *Dispersion de contaminants solides dans le lit d'une rivière*.

References

Agudo, J. and Wierschem, A.: Incipient motion of a single particle on regular substrates in laminar shear flow, Physics of Fluids, 24, 093 302, 2012.

Ancey, C., Davison, A., Bohm, T., Jodeau, M., and Frey, P.: Entrainment and motion of coarse particles in a shallow water stream down a steep slope, J. Fluid Mech., 595, 83–114, doi: 10.1017/S0022112007008 774, 2008.

Berkowitz, B. and Scher, H.: Theory of anomalous chemical transport in random fracture networks, Physical Review E, 57, 5858, 1998.

Blom, A. and Parker, G.: Vertical sorting and the morphodynamics of bed form–dominated rivers: A modeling framework, Journal of Geophysical Research: Earth Surface (2003–2012), 109, 2004.

Bradley, D. N.: Direct Observation of Heavy-Tailed Storage Times of Bed Load Tracer Particles Causing Anomalous Superdiffusion, Geophysical Research Letters, 44, 2017.

Bradley, D. N. and Tucker, G. E.: Measuring gravel transport and dispersion in a mountain river using passive radio tracers, Earth Surface Processes and Landforms, 37, 1034–1045, 2012.

Bradley, D. N., Tucker, G. E., and Benson, D. A.: Fractional dispersion in a sand bed river, Journal of Geophysical Research, 115, F00A09, 2010.

Charru, F.: Selection of the ripple length on a granular bed sheared by a liquid flow, Phys. Fluids, 18, 121 508–1–121 508–9, doi: 0.1017/S002211200500 786X, 2006.

Charru, F., Mouilleron, H., and Eiff, O.: Erosion and deposition of particles on a bed sheared by a viscous flow, Journal of Fluid Mech., 519, 55–80, 2004.

Crickmore, M. and Lean, G.: The measurement of sand transport by means of radioactive tracers, in: Proceedings of the Royal Society of London A: Mathematical, Physical and Engineering Sciences, vol. 266, pp. 402–421, The Royal Society, 1962.

Einstein, H. A.: Bed load transport as a probability problem, in: Sedimentation: 746 Symposium to Honor Professor H.A. Einstein, 1972. translation from 747 German of H.A. Einstein doctoral thesis. Originally presented to Federal Institute of Technology, Zurich, Switzerland, 1937, pp. C1 – C105, 1937.

Fathel, S., Furbish, D., and Schmeeckle, M.: Parsing anomalous versus normal diffusive behavior of bed load sediment particles, Earth Surface Processes and Landforms, 2016.

Fernandez-Luque, R. and Van Beek, R.: Erosion and transport of bed-load sediment, Journal of Hydraulic Research, 14, 127–144, 1976.

Furbish, D., Ball, A., and Schmeeckle, M.: A probabilistic description of the bed load sediment flux: 4. Fickian diffusion at low transport rates, Journal of Geophysical Research, 117, F03 034, 2012a.

Furbish, D., Haff, P., Roseberry, J., and Schmeeckle, M.: A probabilistic description of the bed load sediment flux: 1. Theory, Journal of Geophysical Research, 117, F03 031, 2012b.

Furbish, D., Roseberry, J., and Schmeeckle, M.: A probabilistic description of the bed load sediment flux: 3. The particle velocity distribution and the diffusive flux, Journal of Geophysical Research, 117, F03 033, 2012c.

Furbish, D. J., Fathel, S. L., Schmeeckle, M. W., Jerolmack, D. J., and Schumer, R.: The elements and richness of particle diffusion during sediment transport at small timescales, Earth Surface Processes and Landforms, 2016.

Ganti, V., Meerschaert, M. M., Foufoula-Georgiou, E., Viparelli, E., and Parker, G.: Normal and anomalous diffusion of gravel tracer particles in rivers, Journal of Geophysical Research: Earth Surface, 115, 2010.

Gintz, D., Hassan, M. A., and SCHMIDT, K.-H.: Frequency and magnitude of bedload transport in a mountain river, Earth Surface Processes and Landforms, 21, 433–445, 1996.

Hassan, M. A., Voepel, H., Schumer, R., Parker, G., and Fraccarollo, L.: Displacement characteristics of coarse fluvial bed sediment, Journal of Geophysical Research: Earth Surface, 118, 155–165, 2013.

5 Helley, E. J. and Smith, W.: Development and calibration of a pressure-difference bedload sampler, Geological Survey Open-File Report, December 3, 1971., 1971.

Houssais, M. and Lajeunesse, E.: Bedload transport of a bimodal sediment bed, Journal of Geophysical Research: Earth Surface, 117, 2012.

James, F., Postel, M., and Sepúlveda, M.: Numerical comparison between relaxation and nonlinear equilibrium models. Application to chemical engineering, Physica D: Nonlinear Phenomena, 138, 316–333, 2000.

10 Lajeunesse, E., Malverti, L., and Charru, F.: Bedload transport in turbulent flow at the grain scale: experiments and modeling, J. Geophys. Res. Earth Surface, 115, F04 001, doi:10.1029/2009JF001 628, 2010a.

Lajeunesse, E., Malverti, L., and Charru, F.: Bedload transport in turbulent flow at the grain scale: experiments and modeling, J. Geophys. Res, 115, F04 001, doi:10.1029/2009JF001 628, 2010b.

Lajeunesse, E., Devauchelle, O., Houssais, M., and Seizilles, G.: Tracer dispersion in bedload transport., Adv. Geosci., 37, 1–6, 2013.

15 Lajeunesse, E., Devauchelle, O., Lachaussée, F., and Claudin, P.: Bedload Transport in Laboratory Rivers: The Erosion–Deposition Model, chap. 15, pp. 415–438, John Wiley & Sons Ltd., 2017.

Lenzi, M., Mao, L., and Comiti, F.: Magnitude-frequency analysis of bed load data in an Alpine boulder bed stream, Water Resources Research, 40, 2004.

Leopold, L. B. and Emmett, W. W.: Bedload measurements, East Fork River, Wyoming, Proceedings of the National Academy of Sciences,
20 73, 1000–1004, 1976.

Liébault, F., Bellot, H., Chapuis, M., Klotz, S., and Deschâtres, M.: Bedload tracing in a high-sediment-load mountain stream, Earth Surface Processes and Landforms, 37, 385–399, 2012.

Liu, Y., Metivier, F., Lajeunesse, E., Lancien, P., Narteau, C., and Meunier, P.: Measuring bed load in gravel bed mountain rivers : averaging methods and sampling strategies, Geodynamica Acta, 21, 81–92, doi:10.3166/ga.21.81–92, 2008.

25 Martin, R. L., Jerolmack, D. J., and Schumer, R.: The physical basis for anomalous diffusion in bed load transport, Journal of Geophysical Research, 117, F01 018, 2012.

Nikora, V., Habersack, H., Huber, T., and McEwan, I.: On bed particle diffusion in gravel bed flows under weak bed load transport, Water Resources Research, 38, 17–1, 2002.

Nino, Y. and Garcia, M.: Gravel saltation. Part I: Experiments, Water Resources Research, 30, 1907–1914, 1994.

30 Paola, C., Hellert, P., and Angevine, C.: The large-scale dynamics of grain-size variation in alluvial basins, 1 : theory, Basin Research, 4, 73–90, 1992.

Parker, G., Paola, C., Whipple, K., Mohrig, D., Toro-Escobar, C., Halverson, M., and Skoglund, T.: Alluvial fans formed by channelized fluvial and sheet flow. II: Application, Journal of Hydraulic Engineering, 124, 996–1004, 1998.

Pelosi, A., Parker, G., Schumer, R., and Ma, H.-B.: Exner-Based Master Equation for transport and dispersion of river pebble tracers:
35 Derivation, asymptotic forms, and quantification of nonlocal vertical dispersion, Journal of Geophysical Research: Earth Surface, 119, 1818–1832, 2014.

Phillips, C. and Jerolmack, D.: Dynamics and mechanics of bed-load tracer particles, Earth Surf. Dynam., 2, 513–530, 2014.

Phillips, C. B. and Jerolmack, D. J.: Self-organization of river channels as a critical filter on climate signals, Science, 352, 694–697, 2016.

Phillips, C. B., Martin, R. L., and Jerolmack, D. J.: Impulse framework for unsteady flows reveals superdiffusive bed load transport, Geophysical Research Letters, 40, 1328–1333, 2013.

Roseberry, J., Schmeeckle, M., and Furbish, D.: A probabilistic description of the bed load sediment flux: 2. Particle activity and motions, Journal of Geophysical Research, 117, F03 032, 2012.

5 Sayre, W. and Hubbell, D.: Transport and dispersion of labeled bed material, North Loup River, Nebraska, Tech. Rep. 433-C, U.S. Geol. Surv. Prof. Pap., 1965.

Schumer, R., Meerschaert, M. M., and Baeumer, B.: Fractional advection-dispersion equations for modeling transport at the Earth surface, Journal of Geophysical Research: Earth Surface, 114, 2009.

Seizilles, G., Lajeunesse, E., Devauchelle, O., and Bak, M.: Cross-stream diffusion in bedload transport, Phys. of Fluids, 26, 013 302, 2014.

10 Shields, A. S.: Anwendung der Aehnlichkeitsmechanik und der Turbulenzforschung auf die Geschiebebewegung, Mitteilung der Preussischen Versuchsanstalt fur Wasserbau und Schiffbau, 26, 1936.

Taylor, G.: Dispersion of soluble matter in solvent flowing slowly through a tube, Proceedings of the Royal Society of London. Series A. Mathematical and Physical Sciences, 219, 186–203, 1953.

Turowski, J. M., Yager, E. M., Badoux, A., Rickenmann, D., and Molnar, P.: The impact of exceptional events on erosion, bedload transport

15 and channel stability in a step-pool channel, Earth Surface Processes and Landforms, 34, 1661–1673, 2009.

Turowski, J. M., Badoux, A., and Rickenmann, D.: Start and end of bedload transport in gravel-bed streams, Geophysical Research Letters, 38, 2011.

Van Genuchten, M. T. and Wierenga, P.: Mass transfer studies in sorbing porous media I. Analytical solutions, Soil Science Society of America Journal, 40, 473–480, 1976.

20 Van Rijn, L.: Sediment transport, part I: bed load transport, Journal of hydraulic Engineering, 110, 1431–1456, 1984.

Weeks, E. R. and Swinney, H. L.: Anomalous diffusion resulting from strongly asymmetric random walks, Physical Review E, 57, 4915, 1998.

Zhang, Y., Meerschaert, M. M., and Packman, A. I.: Linking fluvial bed sediment transport across scales, Geophysical Research Letters, 39, 2012.